Geophysical Research Letters

RESEARCH LETTER
10.1029/2019GL083668

Effects of the Compositional Viscosity Ratio on the Long-Term Evolution of Thermochemical Reservoirs in the Deep Mantle

Yang Li[1,2,3], Frédéric Deschamps[4], Jianfeng Yang[2,3], Lin Chen[2,3], Liang Zhao[2,3], and Paul J. Tackley[5]

[1]Key Laboratory of Earth and Planetary Physics, Institute of Geology and Geophysics, Chinese Academy of Sciences, Beijing, China, [2]State Key Laboratory of Lithospheric Evolution, Institute of Geology and Geophysics, Chinese Academy of Sciences, Beijing, China, [3]Institutions of Earth Sciences, Chinese Academy of Sciences, Beijing, China, [4]Institute of Earth Sciences, Academia Sinica, Taipei, Taiwan, [5]Institute of Geophysics, Department of Earth Sciences, ETH Zurich, Zurich, Switzerland

Abstract Numerical experiments of thermochemical mantle convection in 2-D spherical annulus geometry are performed to investigate the effects of compositional viscosity ratio ($\Delta\eta_C$) on the long-term evolution of reservoirs of dense, primordial material in the lowermost mantle of the Earth. The internal heating rate in the primordial material is larger than in the ambient mantle by a factor of 10, accounting for the fact that this material may be enriched in radiogenic elements. We find that if the chemical density contrast is large (128 kg/m^3), $\Delta\eta_C$ plays only a second-order role on the long-term stability of these reservoirs. As the chemical density contrast decreases to smaller values (90 kg/m^3), $\Delta\eta_C$ plays a more significant role. More specifically, when $\Delta\eta_C$ is large, around 10 or larger, convection within the reservoirs of primordial material is less vigorous, which increases the temperature and thermal buoyancy of these structures. This, in turn, can eventually lead them to become unstable, with the majority of the primordial material being advected into the large-scale mantle circulation.

Key Points:
- Large compositional viscosity ratio stabilizes reservoirs of primordial material with large chemical excess density
- Large compositional viscosity ratio destabilizes primordial reservoirs of smaller chemical excess density and large internal heating rate
- Small compositional viscosity ratios do not significantly alter the stability of primordial reservoirs

Supporting Information:
- Supporting Information S1

Correspondence to:
Y. Li and F. Deschamps,
yli@mail.iggcas.ac.cn;
frederic@earth.sinica.edu.tw

Citation:
Li, Y., Deschamps, F., Yang, J., Chen, L., Zhao, L., & Tackley, P. J. (2019). Effects of the compositional viscosity ratio on the long-term evolution of thermochemical reservoirs in the deep mantle. *Geophysical Research Letters*, *46*, 9591–9601. https://doi.org/10.1029/2019GL083668

Received 10 MAY 2019
Accepted 15 AUG 2019
Accepted article online 19 AUG 2019
Published online 31 AUG 2019

1. Introduction

The Earth's deep mantle appears to be heterogeneous at different length scales. The most striking features revealed by seismic observations are two large low shear wave velocity provinces (LLSVPs) located above the core-mantle boundary (CMB) beneath Africa and the Pacific (He & Wen, 2012; Ni et al., 2002; Wang & Wen, 2007). In these regions, the shear wave velocity is slower than in their surroundings by up to a few percent (e.g., Auer et al., 2014; French & Romanowicz, 2015; Masters et al., 2000; Ritsema et al., 2011). The nature and origin of LLSVPs are still enigmatic. Although a purely thermal nature cannot be ruled out (e.g., Davies et al., 2012; Schuberth et al., 2012), several lines of evidence, in particular, from the radial and lateral variations of viscosity ratios (Deschamps & Trampert, 2003; van der Hilst & Kárason, 1999) and from the anticorrelation between shear wave and bulk sound velocities (Ishii & Tromp, 1999; Masters et al., 2000; Trampert et al., 2004) are best explained by a thermochemical nature. Due to mode-coupling approximations, observations based on seismic normal modes data are still ambiguous. Several studies found a density excess in LLSVPs (Ishii & Tromp, 1999; Lau et al., 2017; Moulik & Ekstrom, 2016; Trampert et al., 2004), implying a thermochemical nature for these structures. In contrast, Koelemeijer et al. (2017) found that spherical harmonic degree 2 of Stoneley modes are better explained by light LLSVPs. However, when all structural degrees and other seismic normal modes are taken into account, this preference disappears. Meanwhile, the history of LLSVPs is also poorly constrained. Geochemical signatures of oceanic island basalts (OIBs) indicate the presence of primitive, undegassed mantle materials in the deep mantle (Hofmann, 1997). These reservoirs may have formed very early in Earth's history as a result of mantle differentiation (e.g., Labrosse et al., 2007; Lee et al., 2010) and persisted since then despite mantle convection. Hereafter, we refer to the material composing these reservoirs as primordial material. LLSVPs are a good candidate for such reservoirs, as mantle plumes, from which OIBs originate, apparently rise from their sides or top (e.g., Torsvik et al., 2014). Although their size and shape may have changed in Earth's history, LLSVPs may have been globally stable over long periods of time (e.g., Dziewonski et al., 2010; Torsvik et al., 2014).

Numerical studies of mantle convection have identified important parameters controlling the long-term stability and structure of thermochemical reservoirs. These include the buoyancy ratio (chemical density contrast) and the thermal and compositional viscosity ratios. Buoyancy ratios equivalent to a chemical density contrast around 60–90 kg/m^3 and larger, and a strong dependence of viscosity on temperature (typically, equivalent to global thermal viscosity ratio larger than 10^6) are thought to be key ingredients favoring the long-term stability of LLSVPs (e.g., Deschamps & Tackley, 2008; Li et al., 2014a; McNamara & Zhong, 2004; Mulyukova et al., 2015; Trim & Lowman, 2016). These numerical simulations and laboratory experiments (e.g., Davaille, 1999a, 1999b) further suggest that the compositional viscosity ratio between the dense material and the ambient mantle material plays a substantial, but secondary role.

An estimate of density variations based on tidal tomography (Lau et al., 2017) suggests a much smaller density difference between LLSVPs and the ambient mantle, around 0.5% compared to Preliminary Reference Earth Model (Dziewonski & Anderson, 1981), corresponding to a density excess of about 30 kg/m^3. This value includes the thermal and compositional effects on density, and because LLSVPs are likely hot structures, their effective density contrast compared to their surroundings are necessarily lower than their compositional density contrast. In addition, the observation of Lau et al. (2017) is integrated over a 1,000-km thick layer and may therefore represent an average value between denser LLSVPs from the CMB up to altitudes of a few hundreds of kilometers, and lighter or neutral material at shallower depths. Nevertheless, this finding indicates that the chemical density contrast between LLSVPs and ambient mantle may be lower than previously expected. Meanwhile, the bridgmanite-to-ferropericlase ratio may be higher in LLSVPs than in the surrounding mantle material (Mosca et al., 2012; Trampert et al., 2004), which may cause an increase in the compositional viscosity ratio (Yamazaki & Karato, 2001). This parameter may thus play a more important role than previously thought on deep mantle dynamics and on the stability of thermochemical piles, as suggested by recent numerical simulations (Heyn et al., 2018). For small to moderate chemical density contrasts, this study shows that a higher compositional viscosity ratio helps to stabilize the chemical piles. Another parameter that may influence mantle dynamics and thus requires more detailed and careful examination, is the distribution of internal heating. More specifically, the crystallization of a basal magma ocean may have led to a layer enriched in the main radioactive elements (U and Th) above the CMB (e.g., Corgne et al., 2005). Therefore, if LLSVPs result from such a layer, they may be enriched in heat-producing elements, which could, in turn, affect their long-term evolution (see reviews by McNamara, 2019; Trønnes et al., 2019, and references therein). A possible side effect of increased internal heating is to increase the amount of ^{4}He in LLSVPs (O'Nions & Oxburgh, 1983), as this isotope is a product of the disintegration of U and Th. This would, in turn, reduce the ^{3}He/^{4}He isotopic ratio within LLSVPs, and another reservoir, for instance, bridgmanite-enriched ancient mantle structures (BEAMS; Ballmer et al., 2017), would be needed to explain OIBs helium isotopic ratio. In this study, we extend the studies of Li et al. (2014a) and Heyn et al. (2018) to explore the effects of the compositional viscosity ratio on the long-term stability of reservoirs of dense material assuming a heat-producing ratio between dense material and ambient mantle equal to 10.

2. Method

We performed numerical experiments using the code StagYY (Tackley, 2008), which solves the conservation equations of mass, momentum, energy, and composition for an anelastic compressible fluid with infinite Prandtl number. The model setup is similar to that used by Li et al. (2014a, 2015). Here, we only briefly summarize this setup.

All calculations are performed in 2-D spherical annulus geometry with lateral and radial resolutions of 768 and 96 cells, respectively. The grid is radially refined in the top 100 km and bottom 200 km, with grid refinement reaching, at finest, 6.5 km. We performed resolution tests in which we investigated selected cases with grid size ranging from 512×64 to $1,024 \times 128$, but we did not observe a significant change in the dynamics of our models (Figure S1 in the supporting information). This conclusion was also reached by Lourenço et al. (2016).

We use a tracer ratio method to track the composition field (Tackley & Scott, 2003), with a total number of 2.2 million tracers. This leads to an average number of tracers per cell of about 30, which is enough to model the evolution of the chemical field. Tracers are of two types, modeling the primordial and regular materials, respectively, and the chemical field is determined from the concentration of tracers in each cell, from 0 for a cell containing only regular material, to 1 for a cell containing only primordial material. The primordial

material is set to be denser than the regular mantle material, and the density contrast between primordial and regular materials is controlled by buoyancy ratio (B), which is defined as

$$B = \frac{\Delta\rho_C}{\alpha_s \rho_s \Delta T_S} \tag{1}$$

where $\Delta\rho_C$ is the chemical density contrast between the dense and regular material, α_s and ρ_s are the (reference) surface thermal expansion and density, respectively, and ΔT_S is the superadiabatic temperature difference across the mantle. Note that other studies have used bottom values of thermal expansion and/or density to define the buoyancy ratio. However, provided that the dimensional chemical density contrast is the same, the dynamics of the system should not be affected by the choice of the reference density and the thermal expansion used to define the buoyancy ratio. A basal layer of primordial material with a nondimensional thickness of 0.07 (200 km in dimensional unit) is imposed as initial condition, corresponding to a volume fraction of 3.5%, that is, in the range of initial LLSVPs volume estimated by Hernlund and Houser (2008). The initial temperature field is built by adding small random perturbations to an adiabatic profile with thermal boundary layers at its top and bottom (Figure. S2).

The evolution of the average altitude of primordial material, defined as

$$< H_c >= \frac{1}{V}\int_V C(r,\theta) r \mathrm{d}V, \tag{2}$$

provides a good estimate of mixing efficiency (e.g., Deschamps & Tackley, 2009; Li et al., 2014a). Small values of $< H_c >$, around 0.04 in our case, correspond to stable layering (i.e., the initial layer of primordial material remains unchanged), while large values indicate strong mixing, with complete mixing corresponding to $< H_c >$ around 0.6.

The reference Rayleigh number is defined as

$$Ra_{\mathrm{ref}} = \frac{\alpha_s g \rho_s \Delta T_S D^3}{\eta_0 \kappa_s} \tag{3}$$

where α_s is the surface thermal expansivity, g the acceleration of gravity, and κ_s the surface thermal diffusivity. This reference Rayleigh number is fixed at 10^8 in all experiments.

The viscosity depends on temperature, depth, composition, and yield stress. In addition, we imposed a viscosity jump of 30 between the upper and lower mantles. The viscosity is therefore fully given by

$$\eta = \frac{1}{(\frac{1}{\eta_b(z,T,C)} + \frac{1}{\eta_Y})} \tag{4}$$

with

$$\eta_b(z,T,C) = \eta_0[1 + 29H(z-660)]\exp[E_a \frac{\Delta T_S}{(T+T_{\mathrm{off}})} + V_a \frac{z}{D} + K_a C] \tag{5}$$

and

$$\eta_Y = \frac{\sigma_0 + \sigma_i P}{2\dot{e}} \tag{6}$$

where H is the Heaviside step function, V_a and E_a are the nondimensional activation volume and activation energy, controlling viscosity variations with depth and temperature, K_a is a parameter controlling viscosity variations with composition, and T_{off} is the offset temperature, which determines the viscosity jump through the top thermal boundary layer. Note that the viscosity at the top of the system increases with increasing value of T_{off}. In all our calculations, the value of T_{off} is set to $0.88\Delta T_S$. The yield stress helps to build plate-like behavior at the top of the domain. Here, we defined the yield stress by imposing its surface value σ_0 and its pressure gradient σ_i. In all our simulations, these parameters are set to 200 MPa and 2.5×10^{-3} Pa/Pa, respectively. The yield viscosity η_Y, is defined as the ratio between the yield stress and the second invariant of the strain rate tensor $\dot{e}$. To avoid numerical difficulties, the viscosity is truncated between 10^{-3} and 10^5 of the reference viscosity.

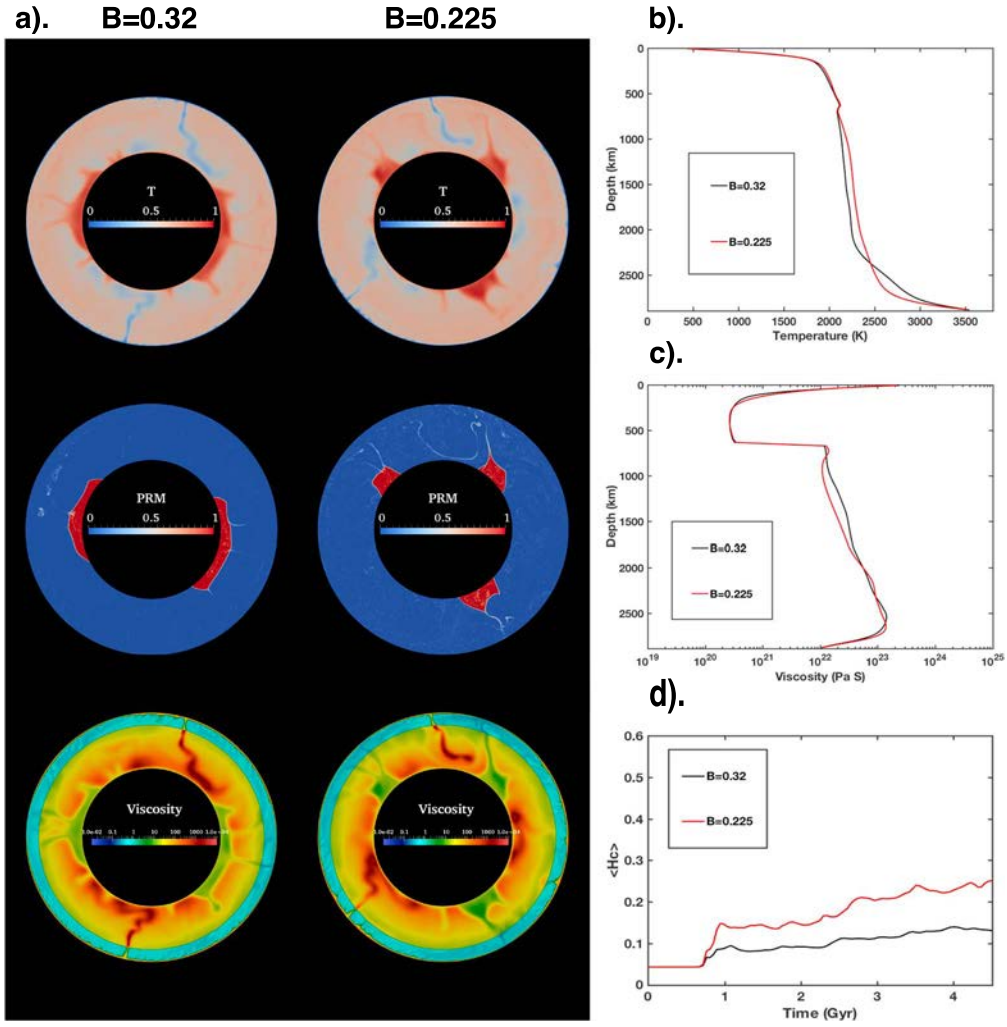

Figure 1. (a) Snapshots of superadiabatic temperature (top), composition (middle), and viscosity (bottom) fields for experiments with $B = 0.32$ (left) and 0.225 (right) at $t = 4.5$ Gyrs; (b) profiles of horizontally averaged temperature at $t = 4.5$ Gyrs; (c) profiles of horizontally averaged viscosity at $t = 4.5$ Gyrs; (d) average altitude of primordial material ($< Hc >$) as a function of time.

The heat-producing elements are assumed to fractionate into the primordial material with a factor Λ. This leads to a distribution of internal heating, Rh, that varies according to the linear relationship

$$Rh(C) = Rh_{\text{ref}} \times [1 + C(\Lambda - 1)] \tag{7}$$

where C is the concentration of dense tracers. The reference internal heating rate is set to 4.0×10^{-12} W/kg in all calculations. Here, taking into account the fact that primordial material may be enriched in radiogenic elements (Kellogg et al., 1999; Richter, 1985), and following Deschamps and Tackley (2008), we set $\Lambda = 10$, that is, the internal heat production in primordial material is increased by a factor of 10 compared to ambient mantle. While this value is somewhat arbitrary and is not constrained by experimental data, it allows to assess the long-term evolution of thermochemical piles enriched in heat-producing elements.

All other physical parameters used in this study are listed in Table S1.

3. Results

We first performed two numerical experiments with buoyancy ratio equal to 0.32 and 0.225, respectively, corresponding to chemical density contrasts of 128 kg/m^3 and 90 kg/m^3. In both simulations, the chemical viscosity ratio is set to 1. Figure 1 shows snapshots from these two experiments taken at $t = 4.5$ Gyrs. Although in both cases, reservoirs of primordial material are maintained in the lower mantle of the Earth,

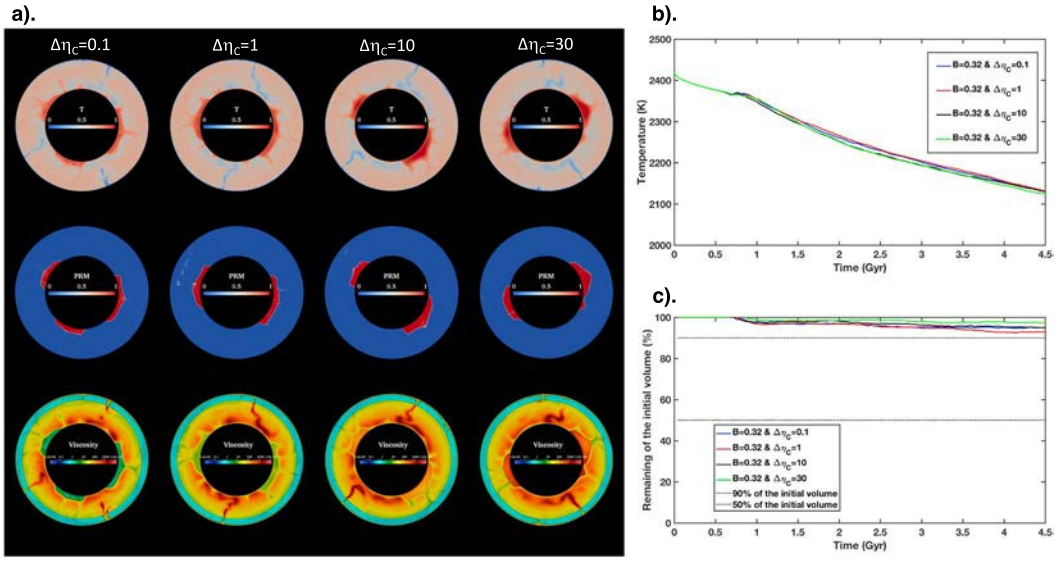

Figure 2. (a) Snapshots of superadiabatic temperature (top), composition (middle), and viscosity (bottom) fields for experiments with $B = 0.32$ and (from left to right) $\Delta\eta_C = 0.1$, 1, 10, 30 at $t = 4.5$ Gyrs; (b) average mantle temperatures as a function of time; (c) fraction of primordial material maintained in large reservoirs as a function of time.

we observe substantial differences in the stability and structures of the reservoirs. For $B = 0.32$, two large stable reservoirs, reaching up to 600 km above CMB, are generated from the deformation of the initial layer of primordial material. Hot plumes are mostly generated at the top and on the margins of these reservoirs. For $B = 0.225$, the primordial layer deforms into three smaller and less stable reservoirs (subsequently referred to as marginally stable), covering a smaller fraction of the CMB area, compared to the case $B = 0.32$, and reaching up to 800 km above the CMB. These smaller, less stable reservoirs experience more thermal erosion through entrainment by plumes, and stronger mixing with the ambient mantle after the onset of convection at 0.8 Gyrs, as indicated by the evolution of the average altitude of primordial material ($< Hc >$; Figure 1d). Figure 1b and 1c show that, for both cases, the profiles of mantle temperature and viscosity are very close to each other. Note that in the lower mantle, the temperature is slightly higher for the case $B = 0.225$, except for the lowermost 500 km, due to the larger size of hot primordial reservoirs in the case with $B = 0.32$. Snapshots of the compositional field (Figure 1a) and the time series of the average altitude of primordial material (Figure 1d) indicate that these two cases are in the stable or marginally stable pile modes. Further hints on the vigor of convection is given by the time evolution of root-mean-square velocity, V_{RMS} (supporting information Figure S3). For cases with $\Delta\eta_C = 1$, V_{RMS} strongly vary in time, but oscillate around 1.5 cm/year after 1 Gyr.

We then performed a series of experiments with $B = 0.32$ and with compositional viscosity ratios between 0.1 and 30. Figure 2a shows snapshots of temperature, composition, and viscosity fields of each of these four simulations at $t = 4.5$ Gyrs. Changing the compositional viscosity ratio from 0.1 to 30 leads to a change of the reservoirs' viscosity, from much lower values than surrounding material at $\Delta\eta_C = 0.1$, to similar, and even larger values at $\Delta\eta_C = 30$. In all cases, the large value of the buoyancy ratio ($B = 0.32$) plays a dominant role in controlling the long-term stability and structure of the primordial reservoirs. Large reservoirs of primordial material remain stable throughout the entire simulations. Slight differences in the size and shape of reservoirs are however visible. In particular, the case with smaller $\Delta\eta_C$ reduces the height of the reservoirs. More generally, the maximum elevation of reservoirs increases slightly with increasing $\Delta\eta_C$. Figure 2b, plotting the evolution of averaged mantle temperature as a function of time, indicates that after the onset of convection at 0.8 Gyrs, all cases experience a similar cooling rate of ~65 K/Gyr. Note that, because our models do not include time-dependent heat sources and do not account for core cooling, this cooling rate is determined by the initial temperature condition and the internal heating rate. Figure 2c shows that over 90% of primordial material is maintained within the large reservoirs over a period of 4.5 Gyrs' evolution. This series of experiments thus demonstrate, in agreement with previous studies (e.g., Deschamps & Tackley, 2009; Li et al., 2014a; McNamara & Zhong, 2004), that if it is large enough, the buoyancy controls

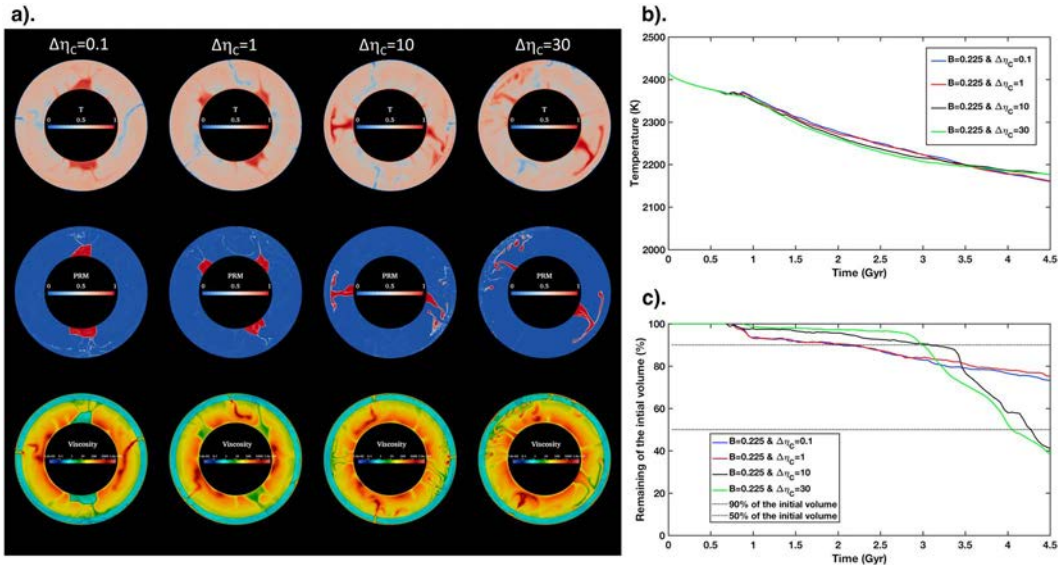

Figure 3. (a) Snapshots of superadiabatic temperature (top), composition (middle), and viscosity (bottom) fields for experiments with $B = 0.225$ and (from left to right) $\Delta\eta_C = 0.1, 1, 10, 30$ at $t = 4.5$ Gyrs; (b) average mantle temperatures as a function of time; (c) fraction of primordial material maintained in large reservoirs as a function of time.

the long-term stability and structure of the reservoirs of primordial material in the lower mantle, while the compositional viscosity ratio plays a secondary role, mainly affecting the height of these structures.

We then performed a second series of experiments in which we decreased the value of the buoyancy ratio to $B = 0.225$ (corresponding to a chemical density contrast of 90 kg/m^3) and again vary the compositional viscosity ratio from 0.1 to 30. For this value of B, we observe important differences in the structure and stability of primordial reservoirs, depending on the compositional viscosity ratio. Figure 3a shows the snapshots of temperature, composition, and viscosity fields of these four cases at $t = 4.5$ Gyrs. In contrast to the results we obtained for $B = 0.32$, the structure and stability of primordial reservoirs strongly vary with the compositional viscosity ratio. For $\Delta\eta_C$ equal to 0.1 and 1, primordial reservoirs form marginally stable piles with high altitude and sometimes sharp edges. For larger values of $\Delta\eta_C$, around 10 and larger, the layer of primordial material is not stable, and wide thermochemical plumes (or "fat plumes") are generated from this layer. This material then spreads laterally and mixes with ambient mantle. As a consequence, the size of the thermochemical reservoir and the fraction of the CMB area covered by primordial material strongly decrease. Figure 3b shows the average mantle temperature as a function of time. Until about 2.0 Gyrs, the cooling rate is about 60 K/Gyr for all cases. At later times, it stays around this value for small $\Delta\eta_C$, but it slightly decreases for cases with larger $\Delta\eta_C$. Again, it is important to keep in mind that the cooling rate is determined by the initial temperature condition and the internal heating rate. Figure 3c shows more details in the evolution of the fraction of primordial material remaining in the midbottom lower mantle. Until about 3.0 or 3.5 Gyrs, the amount of dense material entrained upward is larger for cases with $\Delta\eta_C$ equal to 0.1 and 1 than for cases with larger $\Delta\eta_C$, consistent with previous laboratory (Davaille, 1999a) and numerical (e.g., Heyn et al., 2018) studies. From about 3.0 Gyrs for the case with $\Delta\eta_C = 30$, and 3.5 Gyrs for the case with $\Delta\eta_C = 10$, the fraction of entrained material sharply increases because the primordial reservoirs are no longer stable and, instead, start participating in mantle circulation by forming fat plumes. The size of primordial reservoirs rapidly shrinks, and by the end of the simulation, their size reaches only 40% of their initial volume (Figure 3c). In contrast, for cases with smaller $\Delta\eta_C$, the entrainment remains regular, and the volume of thermochemical piles by the end of the experiments is still about 70% of their initial volume (Figure 3c). One may point out that, while they lead to the destabilization of the reservoirs of primordial material, our simulations with small chemical density contrast and large compositional viscosity ratio predict less efficient mixing between primordial and regular material than observed in previous studies (e.g., Deschamps & Tackley, 2009; Li et al., 2014a; McNamara & Zhong, 2004). Instead, the primordial material spreads laterally after the heads of the piles reach the 660 phase boundary. The large compositional viscosity ratio leads to a slow mixing of the primordial material with the ambient mantle and produces strong small-scale lateral

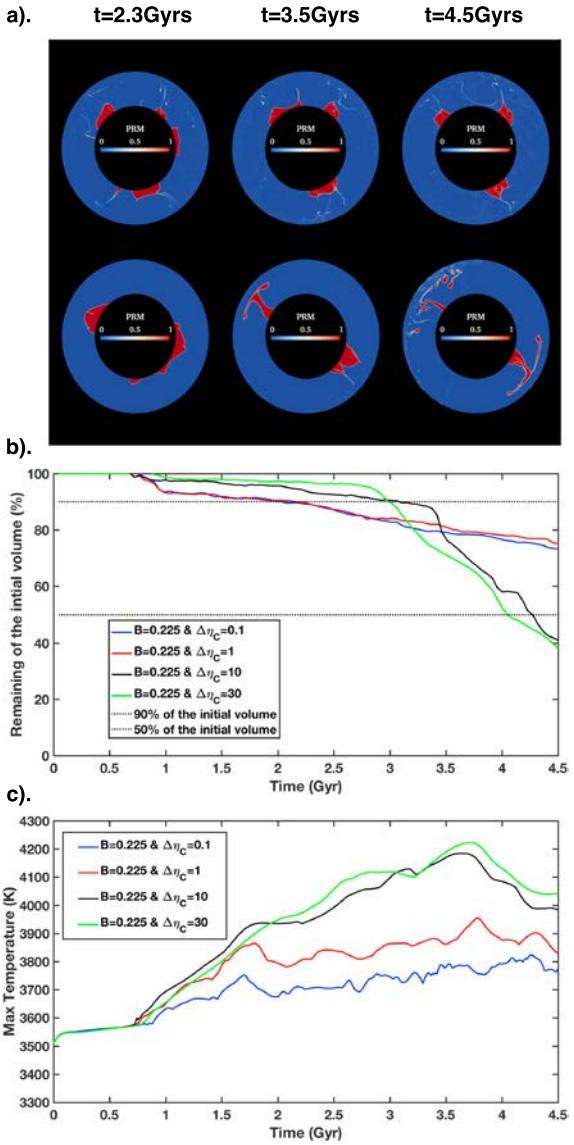

Figure 4. (a) Snapshots of composition fields of $B = 0.225$, $\Delta\eta_C = 1$ (top), 30(bottom) at $t = 2.3$, 3.5, and 4.5 Gyrs; (b) fraction of primordial material maintained in large reservoirs as a function of time; (c) maximum temperature within reservoirs of primordial material as a function of time.

chemical heterogeneities beneath the 660 phase boundary. The main reason is probably that high-viscosity heterogeneities mix far less rapidly (Manga, 1996). In addition, efficiency of mixing may be reduced by differences between the 2-D spherical annulus geometry, which we use in this study, and the 3-D geometry, the later allowing more degrees of freedom. Continuing our simulations beyond 4.5 Gyrs is likely to lead to efficient mixing, as primordial material entrained by fat plumes may be recycled in the deep mantle.

4. Discussion and Conclusions

In this study, we have investigated the effects of compositional viscosity ratio between the primordial and regular mantle materials, $\Delta\eta_C$, on the long-term evolution of mantle dynamics, and on the stability and structure of reservoirs of primordial material in the Earth's lower mantle. Since the primordial material may contain more heat-producing elements and have a larger heat-producing rate compared to the ambient mantle (Kellogg et al., 1999; Richter, 1985), we imposed the heat-producing rate in primordial material to be 1 order of magnitude larger than in regular mantle. We find that the role played by the compositional viscosity ratio is different depending on the values of chemical density contrasts that we tested here, $B = 0.32$ and $B = 0.225$, corresponding to stable and marginally stable reservoirs, respectively.

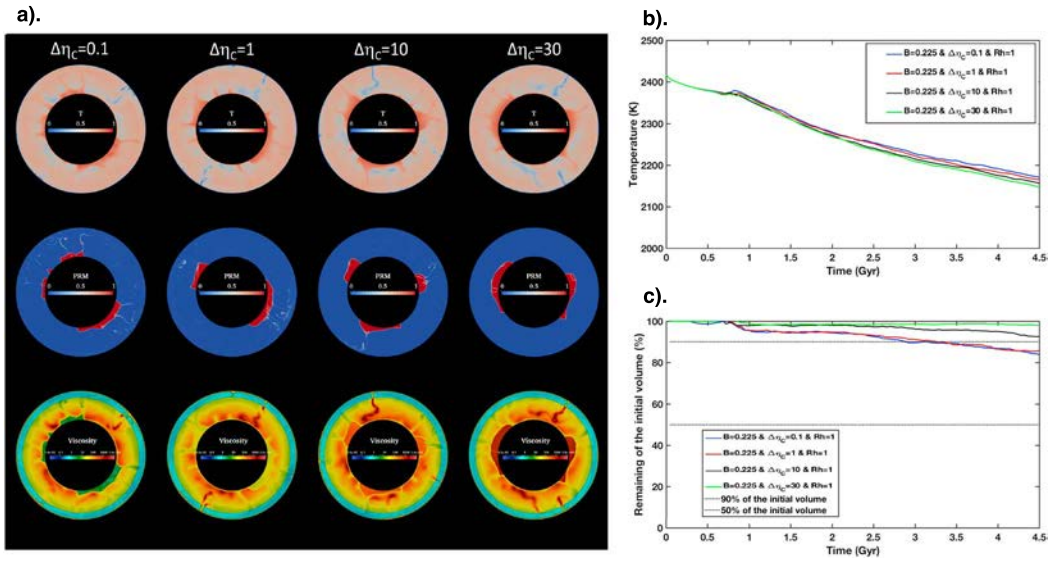

Figure 5. (a) Snapshots of superadiabatic temperature (top), composition (middle), and viscosity (bottom) fields for experiments with $B = 0.225$ and $\Lambda = 1$, (from left to right) $\Delta\eta_C = 0.1$, 1, 10, 30 at $t = 4.5$ Gyrs; (b) averaged mantle temperatures as a function of time; (c) fraction of primordial material maintained in large reservoirs as a function of time.

For large chemical density contrast (128 kg/m^3 in this study), the long-term stability and structure of large primordial reservoirs is not substantially affected by $\Delta\eta_C$. As $\Delta\eta_C$ increases, the viscosity of primordial material increases, thus convection within the reservoirs becomes less vigorous. Due to the large internal heating rate of primordial material, the interiors of these structures become hotter than those obtained with smaller compositional viscosity contrasts. This increases the thermal buoyancy of these reservoirs, tending to destabilize them. For a contrast of 128 kg/m^3, this is manifested by an increase in reservoir height. On the other hand, the large $\Delta\eta_C$ limits the amount of primordial material that is entrained by plumes and mixed with the ambient mantle, thus opposing thermal effects. Nevertheless, a large chemical density contrast is the dominant parameter controlling the stability of large reservoirs of primordial material over long time periods comparable to the history of the Earth, as pointed out in earlier studies (Bower et al., 2013; Deschamps & Tackley, 2009; Li et al., 2014a; Li & McNamara, 2018; McNamara & Zhong, 2004; Mulyukova et al., 2015).

In contrast, for a smaller chemical density contrast (90 kg/m^3 in this study), the stability and structure of primordial reservoirs are strongly affected by $\Delta\eta_C$. For values of this ratio equal to 1 or lower, the primordial material forms marginally stable piles at the base of the mantle, and these piles can persist for a long period of time compared to Earth's history. As $\Delta\eta_C$ increases by 1 order of magnitude or more, reservoirs of primordial material are not stable in the long term. Therefore, in the case of small chemical density contrasts, the compositional viscosity ratio also plays an important role on mantle dynamics, altering the structure and long-term stability of reservoirs of primordial dense material.

Our study reaches a different conclusion than that of Heyn et al. (2018), which suggests that increasing compositional viscosity ratio in simulations with small density contrast has a stabilizing effect on the thermochemical structure. This difference may be caused by the larger internal heat production rate in primordial material that we used in this study. Because of the large $\Delta\eta_C$, the interiors of the reservoirs of primordial material are less vigorous and lose heat less efficiently. Heat accumulation inside these reservoirs results in higher temperature in their interiors (Figure 4c), which enhances their thermal buoyancy and thus reduces their stability. In addition, more viscous compositional piles result in less entrainment by plumes, as suggested by previous studies (e.g., Davaille, 1999a, 1999b; McNamara & Zhong, 2004). These processes finally destabilize the reservoirs of primordial material, and large amounts of this material are entrained upward (Figure 4). To check this hypothesis, we performed additional experiments with $B = 0.225$ and homogeneous heat production rate ($\Lambda = 1$ in equation (3)). Results are shown in Figure 5. In this case, and as expected by our scenario, increasing compositional viscosity ratio helps to stabilize the reservoirs of primordial material and to maintain large amount of this material at the bottom of mantle (Figure 5c), in

agreement with the findings of Heyn et al. (2018). We further note that this case is in very good agreement with similar calculations conducted by Langemeyer et al. (2018). In this study, we implicitly assume that LLSVPs are made of primordial material segregated at the bottom of the mantle as a result of the crystallization of a basal magma ocean, a process that might be long lasting (Labrosse et al., 2007; Trønnes et al., 2019). As a result, the solidification of this magma ocean may have been completed less than three billion years ago. Following our simulations, and if LLSVPs are more viscous than the ambient mantle and enriched in radiogenic elements, they may be at an early stage of their evolution and become unstable in the future. Alternatively, it has been suggested that LLSVPs are made of recycled oceanic crust, in which cases simulations indicate that they could remain stable for billions of years (e.g., Mulyukova et al., 2015). Because the excess density of basalt is assumed to be lower than that presumed for primordial material (e.g., Ballmer et al., 2016), and because basalts are enriched in U and Th (e.g., Corgne et al., 2005; Kellogg et al., 1999), LLSVPs consisting uniquely of basalt may, according to our simulations, become unstable after billions of years of evolution if they are chemically more viscous than the ambient mantle. In summary, by considering a smaller chemical excess density and a higher heat production rate, the compositional viscosity ratio plays a more important and complex role than for the cases with larger chemical excess density and/or similar heat production rate. The properties of the primordial material, including its concentration in radiogenic elements, thus strongly affect the fate of this material. This, in turn, provides some constraints on its nature and origin. If these reservoirs are depleted in heat-producing elements, increasing the compositional viscosity ratio can help in maintaining the stability of these structures over a long period of time. Meanwhile, reservoirs of primordial material with a high heat production in the lower mantle explain the mantle heat budget better (e.g., Jochum et al., 1983; O'Nions & Oxburgh, 1983) and may therefore better explain the long-term thermochemical evolution of Earth's mantle (e.g., Tackley, 2015; van Keken et al., 2001). This, however, might be at the cost of decreasing their stability. One may point out that the value of the increase in the heat production rate we assumed is somehow arbitrary and that the detailed thermochemical structure of the mantle should depend on the exact value of the enrichment of LLSVPs in radiogenic elements. Stronger enrichments, compared to the one we used, may lead to less stable structures, while smaller enrichment may not substantially affect the thermochemical structure. Furthermore, accounting for a decaying heat production rate and for core cooling may affect the long-term stability of the thermochemical structure. Quantifying these factors however requires additional series of experiments. In addition, an exhaustive study should explore a larger range of the buoyancy and compositional viscosity ratios than those we considered. Finally, our findings may be altered by other factors, including a more complex D'' layer with a different viscosity structure. More specifically, the D'' layer may be composed of postperovskite, the viscosity of which may be lower than that of bridgmanite by 2 to 3 orders of magnitude (Ammann et al., 2010). This may, in turn, influence the dynamics of the lower mantle, for instance, allowing a more vigorous convection that may help to extract more heat from the large primordial reservoirs (e.g., Li et al., 2014b). This should be carefully examined in future works.

Acknowledgments
We would like to thank Julian Lowman and an anonymous colleague for their constructive reviews that helped to improve an earlier version of this manuscript. This research was supported by National Natural Science Foundation of China (NSFC) Grants 41888101, 41704100, 41625016, and the Strategic Priority Research Program (B) of Chinese Academy of Sciences, Grant XDB18000000. Y. L. was funded by the CAS Pioneer Hundred Talents Program, Chinese Academy of Sciences. F. D. was funded by Academia Sinica Investigator Award AS-IA-108-M03. The calculations were performed on Tianhe-1(A) at National Supercomputer Center in Tianjin. We note that there are no data-sharing issues since all of the numerical information is provided in the figures produced by solving the equations in the paper and supporting information. Data are available at this site (https://doi.org/10.5281/zenodo.3367504).

References

Ammann, M., Brodholt, J., Wookey, J., & Dobson, D. (2010). First-principles constraints on diffusion in lower-mantle minerals and a weak D" layer. *Nature*, *465*(7297), 462–465. https://doi.org/10.1038/nature09052

Auer, L., Boschi, L., Becker, T. W., Nissen-Meyer, T., & Giardini, D. (2014). Savani: A variable resolution whole-mantle model of anisotropic shear velocity variations based on multiple data sets. *Journal of Geophysical Research: Solid Earth*, *119*, 3006–3034. https://doi.org/10.1002/2013JB010773

Ballmer, M. D., Houser, C., Hernlund, J. W., Wentzcovitch, R. M., & Hirose, K. (2017). Persistence of strong silica-enriched domains in the Earth's lower mantle. *Nature Geoscience*, *10*(3), 236–241. https://doi.org/10.1038/Ngeo2898

Ballmer, M. D., Schumacher, L., Lekic, V., Thomas, C., & Ito, G. (2016). Compositional layering within the large low shear-wave velocity provinces in the lower mantle. *Geochemistry, Geophysics, Geosystems*, *17*, 5056–5077. https://doi.org/10.1002/2016gc006605

Bower, D. J., Gurnis, M., & Seton, M. (2013). Lower mantle structure from paleogeographically constrained dynamic Earth models. *Geochemistry, Geophysics, Geosystems*, *14*, 44–63. https://doi.org/10.1029/2012GC004267

Corgne, A., Liebske, C., Wood, B. J., Rubie, D. C., & Frost, D. J. (2005). Silicate perovskite-melt partitioning of trace elements and geochemical signature of a deep perovskitic reservoir. *Geochimica et Cosmochimica Acta*, *69*(2), 485–496. https://doi.org/10.1016/j.gca.2004.06.041

Davaille, A. (1999a). Simultaneous generation of hotspots and superswells by convection in a heterogeneous planetary mantle. *Nature*, *402*(6763), 756–760.

Davaille, A. (1999b). Two-layer thermal convection in miscible viscous fluids. *Journal of Fluid Mechanics*, *379*, 223–253. https://doi.org/10.1017/S0022112098003322

Davies, D. R., Goes, S., Davies, J., Schuberth, B., Bunge, H.-P., & Ritsema, J. (2012). Reconciling dynamic and seismic models of Earth's lower mantle: The dominant role of thermal heterogeneity. *Earth and Planetary Science Letters*, *353-354*(0), 253–269. https://doi.org/10.1016/j.epsl.2012.08.016

Deschamps, F., & Tackley, P. J. (2008). Searching for models of thermo-chemical convection that explain probabilistic tomography: I. Principles and influence of rheological parameters. *Physics of the Earth and Planetary Interiors*, *171*(1-4), 357–373. https://doi.org/10.1016/j.pepi.2008.04.016

Deschamps, F., & Tackley, P. J. (2009). Searching for models of thermo-chemical convection that explain probabilistic tomography. II. Influence of physical and compositional parameters. *Physics of the Earth and Planetary Interiors*, *176*(1-2), 1–18. https://doi.org/10.1016/j.pepi.2009.03.012

Deschamps, F., & Trampert, J. (2003). Mantle tomography and its relation to temperature and composition. *Physics of the Earth and Planetary Interiors*, *140*(4), 277–291.

Dziewonski, A. M., & Anderson, D. L. (1981). Preliminary reference Earth model. *Physics of the earth and planetary interiors*, *25*(4), 297–356.

Dziewonski, A. M., Lekic, V., & Romanowicz, B. A. (2010). Mantle anchor structure: An argument for bottom up tectonics. *Earth and Planetary Science Letters*, *299*(1-2), 69–79. https://doi.org/10.1016/j.epsl.2010.08.013

French, S. W., & Romanowicz, B. (2015). Broad plumes rooted at the base of the Earth's mantle beneath major hotspots. *Nature*, *525*(7567), 95.

He, Y., & Wen, L. (2012). Geographic boundary of the "Pacific Anomaly" and its geometry and transitional structure in the north. *Journal of Geophysical Research*, *117*, B09308. https://doi.org/10.1029/2012JB009436

Hernlund, J. W., & Houser, C. (2008). On the statistical distribution of seismic velocities in Earth's deep mantle. *Earth and Planetary Science Letters*, *265*(3-4), 423–437.

Heyn, B. H., Conrad, C. P., & Trønnes, R. G. (2018). Stabilizing effect of compositional viscosity contrasts on thermochemical piles. *Geophysical Research Letters*, *45*, 7523–7532. https://doi.org/10.1029/2018GL078799

Hofmann, A. (1997). Mantle geochemistry: The message from oceanic volcanism. *Nature*, *385*(6613), 219–229. https://doi.org/10.1038/385219a0

Ishii, M., & Tromp, J. (1999). Normal-mode and free-air gravity constraints on lateral variations in velocity and density of Earth's mantle. *Science*, *285*(5431), 1231–1236. https://doi.org/10.1126/science.285.5431.1231

Jochum, K. P., Hofmann, A. W., Ito, E., Seufert, H. M., & White, W. M. (1983). K, U and Th in mid-ocean ridge basalt glasses and heat production, K/U and K/Rb in the mantle. *Nature*, *306*(5942), 431–436.

Kellogg, L. H., Hager, B. H., & van der Hilst, R. D. (1999). Compositional stratification in the deep mantle. *Science*, *283*(5409), 1881–1884.

Koelemeijer, P., Deuss, A., & Ritsema, J. (2017). Density structure of Earth's lowermost mantle from Stoneley mode splitting observations. *Nature Communications*, *8*(15), 241.

Labrosse, S., Hernlund, J., & Coltice, N. (2007). A crystallizing dense magma ocean at the base of the Earth's mantle. *Nature*, *450*(7171), 866–869.

Langemeyer, S. M., Lowman, J. P., & Tackley, P. J. (2018). The sensitivity of core heat flux to the modeling of plate-like surface motion. *Geochemistry, Geophysics, Geosystems*, *19*, 1282–1308. https://doi.org/10.1002/2017GC007266

Lau, H. C., Mitrovica, J. X., Davis, J. L., Tromp, J., Yang, H.-Y., & Al-Attar, D. (2017). Tidal tomography constrains Earth's deep-mantle buoyancy. *Nature*, *551*(7680), 321.

Lee, C.-T. A., Luffi, P., Höink, T., Li, J., Dasgupta, R., & Hernlund, J. (2010). Upside-down differentiation and generation of a primordial lower mantle. *Nature*, *463*(7283), 930–933. https://doi.org/10.1038/nature08824

Li, Y., Deschamps, F., & Tackley, P. J. (2014a). The stability and structure of primordial reservoirs in the lower mantle: Insights from models of thermochemical convection in three-dimensional spherical geometry. *Geophysical Journal International*, *199*(2), 914–930. https://doi.org/10.1093/gji/ggu295

Li, Y., Deschamps, F., & Tackley, P. J. (2014b). Effects of low-viscosity post-perovskite on the stability and structure of primordial reservoirs in the lower mantle. *Geophysical Research Letters*, *41*, 7089–7097. https://doi.org/10.1002/2014GL061362

Li, Y., Deschamps, F., & Tackley, P. J. (2015). Effects of the post-perovskite phase transition properties on the stability and structure of primordial reservoirs in the lower mantle of the Earth. *Earth and Planetary Science Letters*, *432*, 1–12. https://doi.org/10.1016/j.epsl.2015.09.040

Li, M., & McNamara, A. K. (2018). The influence of deep mantle compositional heterogeneity on Earth's thermal evolution. *Earth and Planetary Science Letters*, *500*, 86–96. https://doi.org/10.1016/j.epsl.2018.08.009

Lourenço, D. L., Rozel, A., & Tackley, P. J. (2016). Melting-induced crustal production helps plate tectonics on Earth-like planets. *Earth and Planetary Science Letters*, *439*, 18–28.

Manga, M. (1996). Mixing of heterogeneities in the mantle: Effect of viscosity differences. *Geophysical Research Letters*, *23*, 403–406. https://doi.org/10.1029/96GL00242

Masters, G., Laske, G., Bolton, H., & Dziewonski, A. (2000). The relative behavior of shear velocity, bulk sound speed, and compressional velocity in the mantle: Implications for chemical and thermal structure. *Earth's deep interior: Mineral physics and tomography from the atomic to the global scale*, *117*, 63–87. https://doi.org/10.1029/GM117p0063

McNamara, A. K. (2019). A review of large low shear velocity provinces and ultra low velocity zones. *Tectonophysics*, *760*, 199–220. https://doi.org/10.1016/j.tecto.2018.04.015

McNamara, A. K., & Zhong, S. (2004). Thermochemical structures within a spherical mantle: Superplumes or piles? *Journal of Geophysical Research*, *109*, B07402. https://doi.org/10.1029/2003JB002847

Mosca, I., Cobden, L., Deuss, A., Ritsema, J., & Trampert, J. (2012). Seismic and mineralogical structures of the lower mantle from probabilistic tomography. *Journal of Geophysical Research*, *117*, B06304. https://doi.org/10.1029/2011JB008851

Moulik, P., & Ekstrom, G. (2016). The relationships between large-scale variations in shear velocity, density, and compressional velocity in the Earth's mantle. *Journal of Geophysical Research: Solid Earth*, *121*, 2737–2771. https://doi.org/10.1002/2015JB012679

Mulyukova, E., Steinberger, B., Dabrowski, M., & Sobolev, S. V. (2015). Survival of LLSVPs for billions of years in a vigorously convecting mantle: Replenishment and destruction of chemical anomaly. *Journal of Geophysical Research: Solid Earth*, *120*, 3824–3847. https://doi.org/10.1002/2014JB011688

Ni, S., Tan, E., Gurnis, M., & Helmberger, D. (2002). Sharp sides to the African superplume. *Science*, *296*(5574), 1850–1852. https://doi.org/10.1126/science.1070698

O'Nions, R. K., & Oxburgh, E. R. (1983). Heat and helium in the Earth. *Nature*, *306*(5942), 429–431.

Richter, F. M. (1985). Models for the Archean thermal regime. *Earth and Planetary Science Letters*, *73*(2), 350–360. https://doi.org/10.1016/0012-821X(85)90083-4

Ritsema, J., Deuss, A., Van Heijst, H., & Woodhouse, J. (2011). S40RTS: A degree-40 shear-velocity model for the mantle from new Rayleigh wave dispersion, teleseismic traveltime and normal-mode splitting function measurements. *Geophysical Journal International*, *184*(3), 1223–1236.

Schuberth, B. S., Zaroli, C., & Nolet, G. (2012). Synthetic seismograms for a synthetic Earth: Long-period *P*-and *S*-wave traveltime variations can be explained by temperature alone. *Geophysical Journal International*, *188*(3), 1393–1412.

Tackley, P. J. (2008). Modelling compressible mantle convection with large viscosity contrasts in a three-dimensional spherical shell using the Yin-Yang grid. *Physics of the Earth and Planetary Interiors*, *171*(1-4), 7–18. https://doi.org/10.1016/j.pepi.2008.08.005

Tackley, P. (2015). Mantle geochemical geodynamics. In G. Schubert (Ed.), *Treatise on Geophysics* (2nd ed., pp. 521–585). Oxford: Elsevier. https://doi.org/10.1016/B978-0-444-53802-4.00134-2

Tackley, P. J., & Scott, K. D. (2003). Testing the tracer ratio method for modeling active compositional fields in mantle convection simulations. *Geochemistry, Geophysics, Geosystems*, *4*(4), 8302. https://doi.org/10.1029/2001GC000214

Torsvik, T. H., van der Voo, R., Doubrovine, P. V., Burke, K., Steinberger, B., Ashwal, L. D., et al. (2014). Deep mantle structure as a reference frame for movements in and on the Earth. In *Proceedings of the National Academy of Sciences*. https://doi.org/10.1073/pnas.1318135111

Trampert, J., Deschamps, F., Resovsky, J., & Yuen, D. (2004). Probabilistic tomography maps chemical heterogeneities throughout the lower mantle. *Science*, *306*(5697), 853–856. https://doi.org/10.1126/science.1101996

Trim, S. J., & Lowman, J. P. (2016). Interaction between the supercontinent cycle and the evolution of intrinsically dense provinces in the deep mantle. *Journal of Geophysical Research: Solid Earth*, *121*, 8941–8969. https://doi.org/10.1002/2016JB013285

Trønnes, R. G., Baron, M. A., Eigenmann, K. R., Guren, M. G., Heyn, B. H., Løken, A., & Mohn, C. E. (2019). Core formation, mantle differentiation and core-mantle interaction within Earth and the terrestrial planets. *Tectonophysics*, *760*, 165–198. https://doi.org/10.1016/j.tecto.2018.10.021

van Keken, P. E., Ballentine, C. J., & Porcelli, D. (2001). A dynamical investigation of the heat and helium imbalance. *Earth and Planetary Science Letters*, *188*(3), 421–434. https://doi.org/10.1016/S0012-821X(01)00343-0

van der Hilst, R. D., & Kárason, H. (1999). Compositional heterogeneity in the bottom 1000 kilometers of Earth's mantle: Toward a hybrid convection model. *Science*, *283*(5409), 1885–1888.

Wang, Y., & Wen, L. (2007). Geometry and *P* and *S* velocity structure of the "African Anomaly". *Journal of Geophysical Research*, *112*, B05313. https://doi.org/10.1029/2006JB004483

Yamazaki, D., & Karato, S.-I. (2001). Some mineral physics constraints on the rheology and geothermal structure of Earth's lower mantle. *American Mineralogist*, *86*(4), 385–391.